

See discussions, stats, and author profiles for this publication at: <https://www.researchgate.net/publication/231232957>

A Borromean Weave Coordination Polymer Sustained by Urea–Sulfate Hydrogen Bonding and Its Selective Anion Separation Properties

ARTICLE *in* CRYSTAL GROWTH & DESIGN · DECEMBER 2009

Impact Factor: 4.89 · DOI: 10.1021/cg901159r

CITATIONS

35

READS

10

2 AUTHORS, INCLUDING:



Nayarassery Narayanan Adarsh

Catalan Institute of Nanoscience and Nanot...

46 PUBLICATIONS 733 CITATIONS

SEE PROFILE

A Borromean Weave Coordination Polymer Sustained by Urea–Sulfate Hydrogen Bonding and Its Selective Anion Separation Properties

N. N. Adarsh and Parthasarathi Dastidar*

Department of Organic Chemistry, Indian Association for the Cultivation of Science (IACS),
2A & 2B Raja S C Mullick Road, Jadavpur Kolkata – 700032, West Bengal, India

Received September 22, 2009; Revised Manuscript Received November 20, 2009

ABSTRACT: A 3-fold ($2D \rightarrow 2D$) (6,3) Borromean weave coordination polymer sustained by urea–sulfate hydrogen bonding is formed when *N,N'*-bis(3-pyridyl)-*p*-phenylenebisurea (**L1**) is reacted with $\text{ZnSO}_4 \cdot 7\text{H}_2\text{O}$, whereas the corresponding bis-amide derivative *N,N'*-bis(3-pyridyl)terephthalamide (**L2**) gave a coordination polymer displaying a 2D corrugated sheet under the identical reaction conditions; sulfate anion can be selectively separated from a complex mixture of anions (sulfate, nitrate, perchlorate, and triflate) by *in situ* crystallization of these coordination polymers.

Borromean links is a fascinating topology that has inspired human beings, and many such examples exist in history, arts, and science.¹ In the Borromean topology, three closed circuits are entangled in such a fashion that all the entangled components can be separated just by breaking one of the circuits. Nature adopts interpenetration via topological Hopf links (two closed circuits interpenetrated just once, i.e. catenation) in order to achieve close packing to fill the void space in the crystal. The Borromean link is an alternative method of entanglement without a Hopf link. The intriguing feature of the interweaving phenomenon of Borromean is that none of the circuits is catenated to another one but overall they are inseparable (Figure 1).

Borromean topology has been a synthetic goal of interest in molecular form inspired by some theoretical studies.² The first such molecular Borromean link was achieved by DNA nanotechnology in 1997.³ There have been a handful Borromean coordination polymers which were not recognized by the original authors but correctly classified by Carlucci et al. in 2003.⁴ Since then Borromean coordination polymer has become a synthetic goal as it is aesthetically pleasing, intellectually intriguing, synthetically challenging and mechanically strong.^{5–10} Most of the reported examples display $2D \rightarrow 2D$ Borromean entanglement involving 3-fold (6,3) honeycomb layers (*hcb*). More recently, a $2D \rightarrow 2D$ Borromean link involving 3-fold (4,4) sq layers has been reported.¹¹ However, deliberate construction of Borromean network is a daunting task.¹²

The reported Borromean coordination polymeric systems are known to be sustained by various noncovalent interactions such as hydrogen bonding,^{13a} halogen bonding,^{8,13b} $\pi \cdots \pi$ stacking,^{13c} and $\text{Ag} \cdots \text{Ag}$ ^{6,13d} and $\text{Au} \cdots \text{Au}$ ^{13e} interactions in addition to van der Waals contacts. Examination of the reported structures involving (6,3) *hcb* reveals that highly undulating layer structures with large honeycomb cavities, presumably to ensure 3-fold interpenetration and interlayer nonbonded interactions, are some of the criterion for Borromean link formation.

We are interested in coordination polymeric compounds derived from *noninnocent* ligands which are equipped with supramolecular functionalities such as hydrogen bonding. The hydrogen bonding functionalized ligands are capable of interacting with the counteranions, may induce complementary internetwork interactions, and limit the plausible supramolecular architecture of the coordination polymers.¹⁴ In this context, we have been exploiting the hydrogen bonding backbone and ligating topology of the ligands; the specific hydrogen bonding interactions of the counteranions with the ligand backbone lead

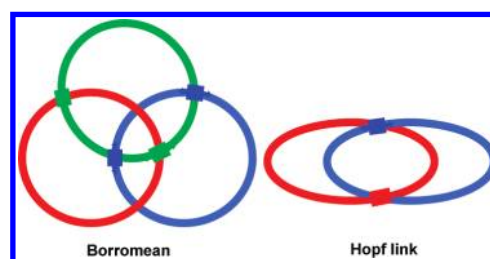


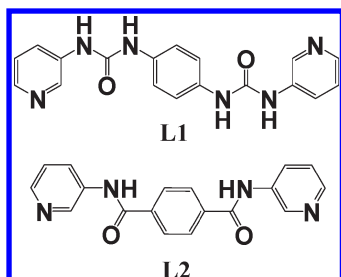
Figure 1. Borromean entanglement and Hopf link.

to the formation of intriguing coordination polymeric systems for material applications such as sorption,¹⁵ inclusion materials,¹⁶ and selective separation of anions.¹⁷ We^{14a,15,18} and others¹⁹ have shown that a urea moiety can interact efficiently with various oxoanions. In fact, in a communication published in the recent past,²⁰ we have exploited urea–sulfate hydrogen bonding interactions to generate a porous self-assembly of nanorods based on a simple coordination polymer.

In this communication, we report the synthesis and single crystal X-ray structures of two coordination polymers, namely $[\{\text{Zn}(\mu\text{-L1})_{1.5}(\text{SO}_4)\} \cdot x\text{H}_2\text{O}]_\infty$ (**1**) and $[\{\text{Zn}(\mu\text{-L2})(\mu\text{-SO}_4)\} \cdot x\text{H}_2\text{O}]_\infty$ (**2**) derived from *N,N'*-bis(3-pyridyl)-*p*-phenylenebisurea (**L1**) and *N,N'*-bis(3-pyridyl)terephthalamide (**L2**). The ditopic ligands **L1** and **L2** equipped with a hydrogen bonding backbone (bis-urea and bis-amide, respectively) have not been exploited in coordination polymers.²⁶ Coordination polymer **1** displays a 3-fold ($2D \rightarrow 2D$) Borromean topology involving a (6,3) *hcb* network, mainly sustained by interlayer urea–sulfate hydrogen bonding and is capable of selectively separating an important anion such as sulfate from a complex mixture of various oxoanions.

Leaf shaped colorless crystals of **1**²⁶ were readily obtained by layering an aqueous methanolic solution of $\text{ZnSO}_4 \cdot 7\text{H}_2\text{O}$ over a DMF solution of **L1** taken in a 1:2 (metal/ligand) molar ratio. The crystal of **1** belongs to the trigonal $R\bar{3}$ space group.²⁷ The asymmetric unit consists of a Zn(II) metal ion, a sulfate counteranion, half of **L1**, and a water molecule; the metal center, the sulfate, and the water molecule were located on a 3-fold symmetry axis whereas the ligand **L1** was located on an inversion center. The counteranion sulfate was found to display rotational disorder around the 3-fold symmetry axis. The metal center Zn(II) displayed a slightly distorted trigonal bipyramidal geometry [$\angle \text{N-Zn-N} = 119.88(2)^\circ$; $\angle \text{N-Zn-O} = 81.7(6) - 109.8(4)^\circ$] wherein the equatorial positions were occupied by the pyridyl N atoms of **L1** and the apical positions were coordinated by the water molecule and O atom of the counteranion sulfate. Extended

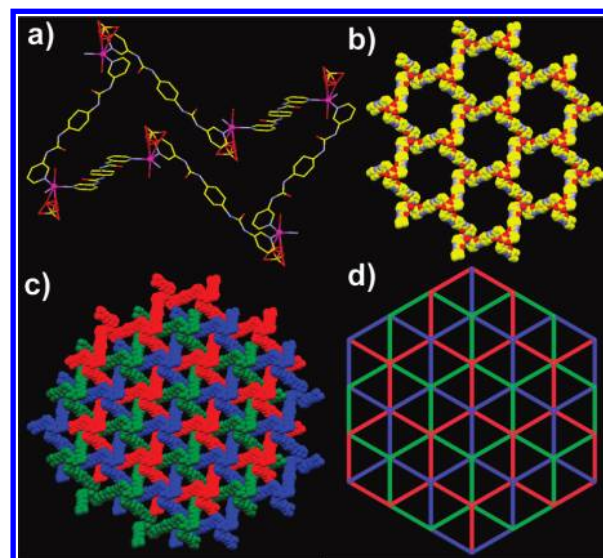
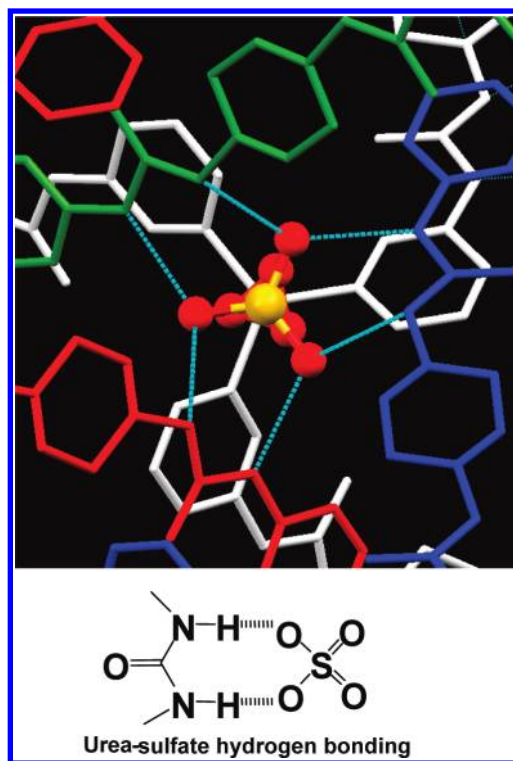
*E-mail: parthod123@rediffmail.com; ocpd@iacs.res.in.

Scheme 1. *syn-anti-syn* and *syn-syn-syn* Conformations of **L1** and **L2**

coordination involving the ligand **L1** in its *syn-anti-syn* conformation (Scheme 1 and Scheme S1 of the Supporting Information) and the metal center in this fashion resulted in the formation of large hexagonal rings having a van der Waals inner diameter of approximately 19.0 Å. The vertices of each hexagon are occupied by Zn(II), and the conformation of each hexagon resembles that of a chair. Extended coordination of this kind ultimately resulted in the formation of a highly undulating 2D honeycomb network involving a (6,3) net. The 2D networks are further packed along the crystallographic *c*-axis, displaying a 3-fold interpenetration without Hopf links, resulting in a Borromean entanglement. TOPOS²¹ analysis suggests that it is a case of 3-fold (2D \rightarrow 2D) Borromean entanglement, as depicted in Figure 2. It is clear from Figure 2 that the green layer is always above the blue layer, which is in turn always above the red layer, which is always above the green layer. It may be noted that no two layers display catenation (Hopf link) but are involved in 3-fold interpenetration. Since the network structure does not have any Hopf link and the entangled 2D layers can be separated just by breaking one of the layers, this network can be categorized as Borromean entanglement. The X-ray structure of **1** also reveals that urea-sulfate hydrogen bonding interactions play a crucial role in stabilizing such Borromean entanglement; sitting on a 3-fold symmetry, three O atoms of the sulfate counteranion were available for hydrogen bonding interactions, and as a result, it indeed formed hydrogen bonding with the three urea moieties coming from three different 2D *hcb* networks [$N \cdots O = 2.62(7) - 2.94(7)$ Å] (Figure 3).

Previously reported Borromean coordination polymers displayed mainly metalophilic (argentophilic^{6,13d} or aurophilic^{13e}) interactions, which were not possible in the present case. Thus, the specific hydrogen bonding between urea and sulfate as discussed above must be one of the most crucial interactions responsible for the stabilization of such a Borromean entanglement. The other examples wherein the Borromean entanglement is sustained by specific hydrogen bonding involving a ligand backbone and counteranions are reported by Steed^{13d} and Vittal.^{13a}

To attain a Borromean entanglement involving a (6,3) *hcb* net, formation of a highly undulating 2D layer is important. From a ditopic ligand such as **L1**, such nonplanar 2D layer formation is dependent on the conformation of the ligand. For example, in the present case (i.e., coordination polymer **1**), the ligand **L1** displayed a *syn-anti-syn* conformation, which ultimately led to the formation of a 2D undulating layer structure via extended coordination with the metal center. We were curious to see what happens if we change the hydrogen bonding backbone of **L1** from bis-urea to bis-amide as in **L2**. Unlike urea-sulfate hydrogen bonding interactions, which display an eight membered hydrogen bonded ring structure (Figure 3), amide-sulfate hydrogen bonding interactions lack structural specificity, displaying less directional $N-H \cdots O$ interactions. Since ligand **L2** can also attain a similar conformation, such as **L1**, and, therefore, can induce the formation of Borromean entanglement, it was considered worthwhile to isolate the reaction product from a reaction between **L2**

**Figure 2.** Crystal structure illustration of **1**: (a) chair conformation of the hexagonal ring; (b) highly undulating (6,3) honeycomb layer; Borromean entanglement (c) in the space filling model and (d) in a TOPOS schematic representation.**Figure 3.** Urea-sulfate hydrogen bonding interactions present in **1**.

and $ZnSO_4 \cdot 7H_2O$ under otherwise identical conditions for synthesizing coordination polymer **1** and to then characterize it by single crystal X-ray diffraction. Thus, block shaped crystals of **2**²⁶ were readily obtained by reacting **L2** and $ZnSO_4 \cdot 7H_2O$ under identical conditions as applied in the case of **1**. The crystals of **2** belong to the noncentric monoclinic space group $P2_1$.²⁷ A fully occupied Zn(II), one molecule of **L1**, one sulfate ion, and one water molecule are located in the asymmetric unit. The metal center Zn(II) displays a slightly distorted tetrahedral geometry [$\angle O-Zn-O = 112.33(12)$; $\angle O-Zn-N = 101.58(14) - 117.10(15)^\circ$] of which two of the

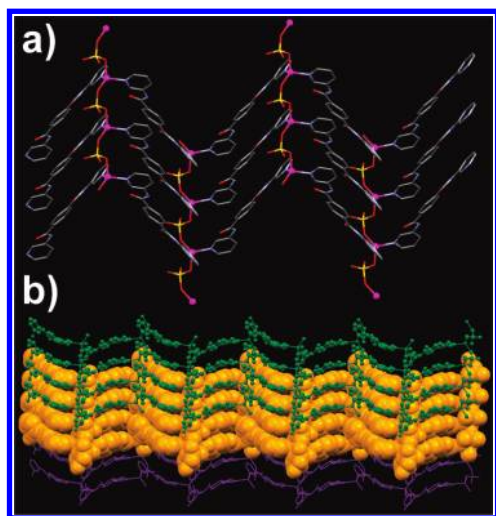


Figure 4. Crystal structure illustration of **2**: (a) 2D corrugated sheet; (b) parallel packing of the 2D sheets.

coordination sites are occupied by the pyridyl N atoms of **L2** and the other two sites are occupied by the O atoms of the sulfate ion and water. Interestingly, the ligand moiety displays a *syn-syn-syn* conformation, unlike its bis-urea counterpart in **1** (Scheme 1 and Scheme S1 of the Supporting Information). As a result of the extended coordination between the ligand **L2** and the adjacent metal center, a 1D zigzag coordination polymeric chain is formed. The 1D chains are further assembled into a 2D corrugated sheet structure by the counteranion sulfate, which acts as a bridging ligand. The 2D sheets are packed on top of each other and are stabilized by hydrogen bonding interactions involving amide N–H and the O atom of the sulfate counteranion [$N\cdots O = 2.904(4)–2.979(5)\text{Å}$, $\angle N–H\cdots O = 152(1)–157(1)^\circ$] (Figure 4).

During the refinement, significant amounts of smeared electron densities were located in the difference Fourier map in both the structures. A SQUEEZE²² calculation indicated the presence of 623 e/unit cell with a solvent accessible area volume of 2723.5 Å³ in **1**. This may be attributed to 10 water molecules in the crystal lattice. Thermogravimetric analysis (TG) also supports this finding; a weight loss of 22.0% within the temperature range 19–272 °C may be assigned to 11 water molecules (1 coordinated + 10 lattice included water molecules; calcd weight loss of 11 water = 22.5%), which is in agreement with the single crystal structure and SQUEEZE results (Figure S1 of the Supporting Information).

The overall packing displays tiny channels running down the crystallographic *a*-axis wherein some disordered electron densities were located in the refinement cycles of **2**. These electron densities were attributed to disordered water molecules and squeezed out in the final cycles of refinement. SQUEEZE calculations showed the presence of 13 e/unit cell (with a solvent accessible area volume of 57.3 Å³), which amounts to 6.5 e per asymmetric unit; this may be attributed to 0.65 water molecule. Since the data were collected at room temperature, loss of lattice-included solvent such as water in the present case may take place. TG data further support this assignment. In TG, a weight loss of 2.6% is observed within the temperature range 24–185 °C whereas the calculated weight loss considering 0.65 water molecule in the asymmetric unit as suggested in the SQUEEZE calculation is 2.4%, which is in agreement with the experimental results (Figure S2 of the Supporting Information).

One of the important aspects of metal–organic hybrid compounds such as coordination polymers is the ability to exchange anions.²³ It has already been demonstrated that metal–organic

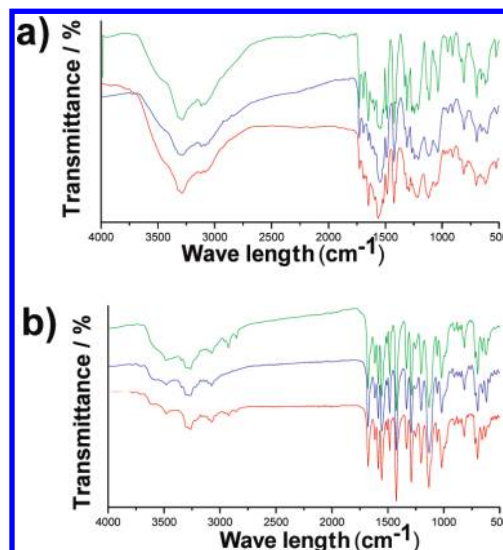


Figure 5. FT-IR comparison plots of (a) **1** and (b) **2** recorded under various conditions: noncompetitive condition (red); condition I (blue); condition II (green).

systems can be exploited to recognize and separate important anions.^{24,17} Recently, *in situ* crystallization of coordination polymers has been proposed to be a viable method to separate a targeted anion from a complex mixture of anions,²³ wherein the organic linker and metal salts having various counteranions are allowed to crystallize together. Since sulfate is an important anion to be separated,²⁵ we carried out systematic studies of anion separation using *in situ* crystallization of **1** and **2** under competitive conditions as described below.

Sulfate, perchlorate, nitrate, and triflate as Zn(II) salts were selected for this study. Two different experiments for each metal–organic system (namely **1** and **2**) were adopted. In the first experiment (condition I), the ligand was reacted with a mixture of Zn(II) salts having different oxoanions in the molar ratio of 2:1 (ligand:metal). In the other experiment (condition II), the reaction was performed using 2:1:2 (ligand:ZnSO₄:Zn–other oxoanions). In all the experiments, the experimental conditions (solvents, temperature, etc.) were kept unchanged, as in the synthesis of **1** and **2** (for details, see the Supporting Information). The reaction products obtained in these experiments were characterized by using X-ray powder diffraction (XRPD), FT-IR, elemental analysis, and energy dispersive X-ray spectrometry (EDX). It is clear from Figure 5 that the FT-IR spectra recorded under various conditions are nearly identical. A strong and broad band at 1116 and 1132 cm^{−1} in the FT-IR data of **1** and **2**, respectively, indicates the presence of sulfate anion ($\nu_{\text{asym}} \text{S–O}$) (Table S1 of the Supporting Information). These results indicate that the coordination polymers **1** and **2** were crystallized out exclusively in the presence of other oxoanions. Both elemental analysis and EDX also support these findings (Table S2 and Figures S3 and S4 of the Supporting Information). Finally, the nearly identical XRPD patterns recorded under various conditions as depicted in the Figure 6 strongly support the selective separation of sulfate as the corresponding coordination polymers **1** and **2** from a complex mixture of oxoanions. It may be noted here that the reaction of both **L1** and **L2** with Zn(II) salts (in separate experiments) having various counteranions such as nitrate, perchlorate, and triflate resulted in crystallization of free ligands, which indicated less reactivity of these ligands toward these metal salts. However, in the presence of a mixture of Zn(II) salts having various counteranions such as sulfate, nitrate, perchlorate, and triflate, only **1** and **2** were separated out as neat crystals, which was advantageous in separating sulfate from a complex mixture. This could be due to both less reactivity

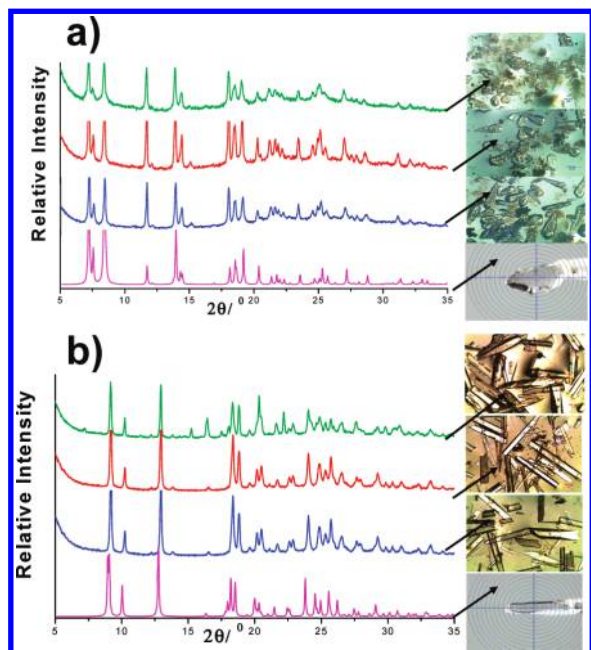


Figure 6. XRPD of (a) **1** and (b) **2** recorded under various conditions: simulated (magenta); as synthesized bulk (blue); condition I (red); condition II (green). The corresponding optical micrographs of the crystals are shown on the right-hand side of the figure.

of these ligands toward these metal salts and weaker hydrogen bonding interactions with the ligand backbone (urea and amide).

Thus, we have reported one of the rare examples of a Borromean coordination polymer (**1**) mainly sustained by urea–sulfate hydrogen bonding interactions. This Borromean entanglement in **1** is devoid of any metallophilic interactions which are the main stabilizing factors in the other reported Borromean structures.^{5,13d} Interestingly, the bis-amide ligand **L2** failed to produce a Borromean topology, which could be due to the *syn–syn–syn* conformation of **L2** as well as the less directional amide–sulfate hydrogen bonding interactions compared to that of urea–sulfate. Most interestingly, both the coordination polymers **1** and **2** could be exploited to separate selectively an important anion sulfate from a complex mixture of various oxoanions such as sulfate, nitrate, perchlorate, and triflate via *in situ* crystallization of the corresponding coordination polymers.

Acknowledgment. We thank the Department of Science & Technology (DST), New Delhi, India, for financial support. N. N.A thanks IACS for research fellowships. Single crystal X-ray diffraction was performed at the DST-funded National Single Crystal Diffractometer Facility at the Department of Inorganic Chemistry, IACS. We are thankful to Prof. Vladislav A. Blatov, and Prof. Davide M. Proserpio for fruitful discussions during the time of manuscript preparation.

Supporting Information Available: Hydrogen bonding parameters for **1** and **2**, Scheme S1, TG (Figures S1 and S2), experimental details for anion separation studies, FT-IR (Table S1), elemental analysis (Table S2), EDX (Figures S3 and S4), and CIF data for **1** and **2**. This material is available free of charge via the Internet at <http://pubs.acs.org>.

References

- (1) (a) Cantrill, S. J.; Chichak, K. S.; Peters, A. J.; Stoddart, J. F. *Acc. Chem. Res.* **2005**, *38*, 1. (b) Seeman, N. C. *Angew. Chem., Int. Ed.* **1998**, *37*, 3220. (c) Siegel, J. S. *Science* **2004**, *304*, 1256. (d) Schalley, C. A. *Angew. Chem., Int. Ed.* **2004**, *43*, 4399. (e) Chichak, K. S.; Cantrill, S. J.; Pease, A. R.; Chiu, S.-H.; Cave, G. W. V.; Atwood, J. L.; Stoddart, J. F. *Science* **2004**, *304*, 1308.
- (2) Liang, C.; Mislow, K. *J. Math. Chem.* **1994**, *16*, 27.
- (3) Mao, C.; Sun, W.; Seeman, N. C. *Nature* **1997**, *386*, 137.
- (4) Carlucci, L.; Ciani, G.; Proserpio, D. M. *CrystEngComm* **2003**, *5*, 269.
- (5) Dobrzanska, L.; Raubenheimer, H. G.; Barbour, L. J. *Chem. Commun.* **2005**, 5050.
- (6) Zhang, X. L.; Guo, C. P.; Yang, Q. Y.; Wang, W.; Liu, W. S.; Kang, B. S.; Su, C. Y. *Chem. Commun.* **2007**, 4242.
- (7) Zhang, X. L.; Guo, C. P.; Yang, Q. Y.; Lu, T. B.; Tong, Y. X.; Su, C. Y. *Chem. Mater.* **2007**, *19*, 4630.
- (8) Liantonio, R.; Metrangolo, P.; Meyer, F.; Pilati, T.; Navarrini, W.; Resnati, G. *Chem. Commun.* **2006**, 1819.
- (9) Li, J.; Song, L.; Du, S. W. *Inorg. Chem. Commun.* **2007**, *10*, 358.
- (10) Lu, X. Q.; Pan, M.; He, J. R.; Cai, Y. P.; Kang, B. S.; Su, C. Y. *CrystEngComm* **2006**, *8*, 827.
- (11) Yao, Q.-X.; Jin, X.-H.; Ju, Z.-F.; Zhang, H.-X.; Zhang, J. *CrystEngComm* **2009**, *11*, 1502.
- (12) Men, Y.-B.; Sun, Junliang.; Huang, Z.-T.; Zheng, Q.-Y. *Angew. Chem., Int. Ed.* **2009**, *48*, 2873.
- (13) (a) Muthu, S.; Yip, J. H. K.; Vittal, J. J. *J. Chem. Soc., Dalton Trans.* **2002**, 4561. (b) Liantonio, R.; Metrangolo, P.; Pilati, T.; Resnati, G. *Cryst. Growth Des.* **2003**, *3*, 355. (c) Suh, M. P.; Choi, H. J.; So, S. M.; Kim, B. M. *Inorg. Chem.* **2003**, *42*, 676. (d) Byrne, P.; Lloyd, G. O.; Clarke, N.; Steed, J. W. *Angew. Chem., Int. Ed.* **2008**, *47*, 5761. (e) Leznoff, D. B.; Xue, B.-Y.; Batchelor, R. J.; Einstein, F. W. B.; Patrick, B. O. *Inorg. Chem.* **2001**, *40*, 6026.
- (14) (a) Krishna Kumar, D.; Jose, D. A.; Das, A.; Dastidar, P. *Inorg. Chem.* **2005**, *44*, 6933. (b) Krishna Kumar, D.; Das, A.; Dastidar, P. *CrystEngComm* **2007**, *9*, 548. (c) Krishna Kumar, D.; Das, A.; Dastidar, P. *Cryst. Growth Des.* **2007**, *7*, 2096.
- (15) Krishna Kumar, D.; Das, A.; Dastidar, P. *CrystEngComm* **2006**, *8*, 805.
- (16) Krishna Kumar, D.; Das, A.; Dastidar, P. *Inorg. Chem.* **2007**, *46*, 7351.
- (17) (a) Adarsh, N. N.; Krishna Kumar, D.; Dastidar, P. *CrystEngComm* **2008**, *10*, 1565. (b) Adarsh, N. N.; Krishna Kumar, D.; Dastidar, P. *CrystEngComm* **2009**, *11*, 796.
- (18) (a) Krishna Kumar, D.; Das, A.; Dastidar, P. *New J. Chem.* **2006**, *30*, 1267. (b) Adarsh, N. N.; Krishna Kumar, D.; Dastidar, P. *Cryst. Growth Des.* **2009**, *9*, 2979.
- (19) (a) Custelcean, R.; Moyer, B. A.; Bryantsev, V. S.; Hay, B. P. *Cryst. Growth Des.* **2006**, *6*, 555. (b) Turner, D. R.; Smith, B.; Spencer, E. C.; Goeta, A. E.; Evans, I. R.; Tocher, D. A.; Howard, J. A. K.; Steed, J. W. *New J. Chem.* **2005**, *29*, 90. (c) Turner, D. R.; Spencer, E. C.; Howard, J. A. K.; Tocher, D. A.; Steed, J. W. *Chem. Commun.* **2004**, 1352. (d) Turner, D. R.; Smith, B.; Goeta, A. E.; Evans, I. R.; Tocher, D. A.; Howard, J. A. K.; Steed, J. W. *CrystEngComm* **2004**, *6*, 633. (e) Custelcean, R.; Bosano, J.; Bonnesen, P. V.; Kertesz, V.; Hay, B. P. *Angew. Chem., Int. Ed.* **2009**, *48*, 4025. (f) Gale, P. A.; Hiscock, J. R.; Moore, S. J.; Caltagirone, C.; Hursthouse, M. B.; Light, M. E. *Chem. Asian J.* **2010**, <http://dx.doi.org/10.1002/asia.200900230>. (g) Caltagirone, C.; Gale, P. A.; Hiscock, J. R.; Brooks, S. J.; Hursthouse, M. B.; Light, M. E. *Chem. Commun.* **2008**, 3007. (h) Caltagirone, C.; Hiscock, J. R.; Hursthouse, M. B.; Light, M. E.; Gale, P. A. *Chem. Eur. J.* **2008**, *14*, 10236. (i) Custelcean, R.; Jiang, De-en; Hay, B. P.; Luo, W.; Gu, B. *Cryst. Growth Des.* **2008**, *8*, 1909.
- (20) Krishna Kumar, D.; Das, A.; Dastidar, P. *Cryst. Growth Des.* **2007**, *7*, 205.
- (21) Blatov, V. A.; Proserpio, D. M. *TOPOS 4.0*, A program package for multipurpose Crystallochemical analysis.
- (22) Van der Sluis, P.; Spek, A. L. *Acta Crystallogr., Sect. A* **1990**, *46*, 194.
- (23) Custelcean, R.; Moyer, B. A. *Eur. J. Inorg. Chem.* **2007**, 1321.
- (24) (a) Custelcean, R.; Remy, P. *Cryst. Growth Des.* **2009**, *9*, 1985. (b) Custelcean, R.; Sellin, V.; Moyer, B. A. *Chem. Commun.* **2007**, 1541. (c) Vilar, R. *Eur. J. Inorg. Chem.* **2008**, 357. (d) Uemura, K.; Kumamoto, Y.; Kitagawa, S. *Chem.—Eur. J.* **2008**, *14*, 9565. (e) Wu, B.; Liang, J.; Yang, J.; Jia, C.; Yang, X.-J.; Zhang, H.; Tang, N.; Janiak, C. *Chem. Commun.* **2008**, 1762. (f) Muthu, S.; Yip, J. H. K.; Vittal, J. J. *J. Chem. Soc., Dalton Trans.* **2002**, 4561. (g) Blondeau, P.; van der Lee, A.; Barboiu, M. *Inorg. Chem.* **2005**, *44*, 5649. (h) Amendola, V.; Boiocchi, M.; Colasson, B.; Luigi, F. *Inorg. Chem.* **2006**, *45*, 6138. (i) Bondy, C. R.; Gale, P. A.; Loeb, S. J. *J. Am. Chem. Soc.* **2004**, *126*, 5030. (j) Su, C.-Y.; Cai, Y.-P.; Chen, C.-L.; Zhang, H.-X.; Kang, B.-S. *J. Chem. Soc., Dalton Trans.* **2001**, 359. (k) Tzeng, B.-C.; Chen, B.-S.; Lee, S.-Y.; Liu, W.-H.; Leeb, G.-H.; Peng, S.-M. *New J. Chem.* **2005**, *29*, 1254. (l) Vilar, R. *Struct. Bonding (Berlin)* **2008**, *129*, 175.

- (25) (a) Lumetta, G. J. The Problem with Anions in the DOE Complex. In *Fundamental and Applications of Anion Separations*; Moyer, B. A., Singh, R. P., Eds.; Kluwer Academic: New York, 2004. (b) Moyer, B. A.; Delmau, L. H.; Fowler, C. J.; Ruas, A.; Bostick, D. A.; Sessler, J. L.; Katayev, E.; Pantos, G. D.; Llinares, J. M.; Hossain, M. A.; Kang, S. O.; Bowman-James, K. In *Supramolecular Chemistry of Environmentally Relevant Anions, in Advances in Inorganic Chemistry*; Vol. 59: Template Effects and Molecular Organization; van Eldik, R., Bowman-James, K., Eds.; Elsevier: Oxford, 2007; p 175. (c) Sessler, J. L.; Katayev, E.; Pantosa, G. D.; Ustynyuk, Y. A. *Chem. Commun.* **2004**, 1276.
- (26) Syntheses of **L1** and **L2**: The syntheses of **L1** and **L2** were reported in the context of organic crystal engineering. Byrne, P.; Turner, D. R.; Lloyd, G. O.; Clarke, N.; Steed, J. W. *Cryst. Growth Des.* **2008**, 8, 3335 for **L1**. Rajput, L.; Singh, S.; Biradha, K. *Cryst. Growth Des.* **2007**, 7, 2788 for **L2**. However, we have followed different methods to synthesize both the ligands, which are as follows. **L1**: To a stirring solution of 3-aminopyridine (686 mg, 7.29 mmol) and triethylamine (3 mL) in 100 mL of anhydrous dichloromethane (DCM) at ice cold temperature under an inert atmosphere was added triphosgene (900 mg, 3.030 mmol), and the solution was kept stirring for 20 min. *p*-Phenylene diamine (394 mg, 3.65 mmol) in 50 mL of dry DCM was then added dropwise. The pale yellow colored solution became a thick brown precipitate, which was further stirred at room temperature for 24 h. After filtration, the precipitate was washed with DCM, air dried, and treated with a 5% NaHCO₃ solution. The resultant solid was filtered, washed with distilled water, and dried. The crude product thus obtained was then dissolved in DMSO, and further addition of distilled water gave **L1** as a gelly precipitate, which was then filtered, washed with excess water, and air dried (700 mg, 55% yield). mp 280–282 °C. Anal. Calcd for C₁₈H₁₆N₆O₂ (%): C, 62.06; H, 4.63; N, 24.12. Found: C, 62.42; H, 4.42; N, 24.14. ¹H NMR (300 MHz, DMSO-*d*₆): δ = 8.79 (2H, s, N-H), 8.69 (2H, s, N-H), 8.60 (2H, s, Py-H), 8.19–8.17 (2H, d, *J* = 4.1 Hz, Py-H), 7.95–7.93 (2H, d, *J* = 7.0 Hz, Py-H), 7.39 (4H, s, Ar-H), 7.33–7.28 (2H, dd, *J* = 4.68, 8.22 Hz, Py-H) ppm. FT-IR (KBr pellet): 3286 (s, urea ν N-H), 3178w, 3126 (m, aromatic ν C-H), 3080w, 3041m, 3024m, 2926w, 1894w, 1693m, 1647 (s, urea ν C=O), 1597 (s, urea δ N-H), 1566s, 1514s, 1479s, 1419s, 1404s, 1327m, 1305s, 1284s, 1247m, 1228s, 1188s, 1120w, 1103w, 1024w, 935w, 898w, 848m, 812m, 765w, 746w, 702s, 669w, 624w, 613w, 588w, 526m cm⁻¹. HRMS calcd for C₁₈H₁₆N₆O₂ [M + H]⁺: 349.1368; found: 349.2404. **L2**: To a solution of 3-aminopyridine (1.069 g, 11.38 mmol) and triethylamine (8 mL) in 80 mL of dry THF under ice cold conditions under a nitrogen atmosphere, terephthaloyl chloride (1.1 g, 5.42 mmol) in dry THF (20 mL) was added dropwise. The thick white colored precipitate thus formed was kept stirring with reflux for 8 h. After filtration, the precipitate was washed with THF, air dried, and treated with 5% NaHCO₃ solution. It was then washed in distilled water, dried, and recrystallized from DMSO (yield: 1.2 g, 70%). Anal. Calcd for C₁₈H₁₄N₄O₂ (%): C, 67.91; H, 4.43; N, 17.60. Found: C, 67.47; H, 4.40; N, 17.86. ¹H NMR (200 MHz, DMSO-*d*₆): δ = 10.64 (2H, s, N-H), 8.98 (2H, s, Py-H), 8.37–8.34 (2H, d, *J* = 9 Hz, Py-H), 8.25–8.22 (2H, d, *J* = 9 Hz, Py-H), 8.15 (4H, s, Ar-H), 7.47–7.40 (2H, dd, *J* = 4.6, 8.2 Hz, Py-H) ppm. FT-IR (KBr pellet): 3346 (s, amide ν N-H), 3265s, 3047 (m, aromatic ν C-H), 1679 (s, amide ν C=O), 1652s, 1618 (s, amide δ N-H), 1562s, 1527s, 1483s, 1415s, 1334s, 1317m, 1284s, 1259w, 1234w, 1190w, 1105w, 1029w, 889w, 865w, 833w, 798w, 702w, 638w, 621w, 540w, 507w cm⁻¹. HRMS calcd for C₁₈H₁₄N₄O₂ [M + H]⁺: 319.2; found: 319.4. **1** was synthesized by layering an aqueous methanolic solution of ZnSO₄·7H₂O (17 mg, 0.059 mmol) over a DMF solution of **L1** (41 mg, 0.118 mmol). After three days, X-ray quality crystals were obtained by a slow evaporation technique. Yield: 77% (40 mg, 0.046 mmol). Anal. Calcd for C₂₇H₂₆N₉O₈SZn·8H₂O (%): C, 38.33; H, 5.00; N, 14.90. Found: C, 38.72; H, 4.76; N, 15.33. FT-IR (KBr pellet): 3286 (s, amide ν N-H), 3085 (m, aromatic ν C-H), 1728 (s, urea ν C=O), 1691 (s, urea δ N-H), 1649s, 1595s, 1562s, 1515m, 1483s, 1423s, 1292s, 1228s, 1213s, 1118 (s, SO₄²⁻ ν_{asym} S-O), 1060m, 906w, 810m, 698s, 651s, 524m cm⁻¹. **2** was synthesized by layering an aqueous methanolic solution of ZnSO₄·7H₂O (18 mg, 0.063 mmol) over a DMF solution of **L2** (40 mg, 0.126 mmol). After one week, X-ray quality crystals were obtained by a slow evaporation technique. Yield: 66% (20 mg, 0.041). Anal. Calcd for C₁₈H₁₄N₄O₆SZn (%): C, 45.06; H, 2.94; N, 11.68. Found: C, 44.88; H, 2.76; N, 12.20. FT-IR (KBr pellet): 3267 (m, amide ν N-H), 3076 (m, aromatic ν C-H), 1677 (s, amide ν C=O), 1614 (s, amide δ N-H), 1585s, 1554s, 1508s, 1483s, 1425s, 1332s, 1290s, 1253w, 1203s, 1132 (sb, SO₄²⁻ ν_{asym} S-O), 1060m, 1018s, 904w, 817m, 719m, 698m, 657m, 626m cm⁻¹.
- (27) X-ray crystallography: X-ray single crystal data were collected using Mo Kα (λ = 0.7107 Å) radiation on a BRUKER APEX II diffractometer equipped with a CCD area detector. Data collection, data reduction, and structure solution/refinement were carried out using the software package of SMART APEX. All structures were solved by direct methods and refined in a routine manner. In most of the cases, non-hydrogen atoms were treated anisotropically. Whenever possible, the hydrogen atoms were located on a difference Fourier map and refined. In other cases, the hydrogen atoms were geometrically fixed. CCDC (CCDC No: 748201 and 748202) contains the supplementary crystallographic data for this paper. These data can be obtained free of charge via www.ccdc.cam.ac.uk/contents/retrieving.html (or from the Cambridge Crystallographic Data Centre, 12 Union Road, Cambridge CB21EZ, U.K. Fax: (+44) 1223-336-033. E-mail: deposit@ccdc.cam.ac.uk). Crystal data for **1**: C₂₇H₂₆N₉O₈SZn, FM = 702.00, trigonal space group R3̄ (No. 148), *a* = 15.0798(19), *b* = 15.0798(19), *c* = 35.075(9) Å. *V* = 6907(2) Å³, *T* = 100 K, *Z* = 6. *D*_c = 1.013 g cm⁻³. *F*(000) = 2166, λ(Mo Kα) = 0.71073 Å, μ = 0.622 mm⁻¹, 2θ_{max} = 41.46°, 7580 collected reflections measured, 1588 observed (*I* > 2σ(*I*)) 163 parameters; *R*_{int} = 0.0367, *R*₁ = 0.0866; *wR*₂ = 0.2358 (*I* > 2σ(*I*)), *R*₁ = 0.0970; *wR*₂ = 0.2462 (all data) with GOF = 1.087. Crystal data for **2**: C₁₈H₁₄N₄O₆SZn, FM = 479.76, monoclinic, space group P2₁ (no. 4), *a* = 4.9904(17), *b* = 19.473(7), *c* = 9.891(3) Å. β = 93.762(5)°. *V* = 959.1(6) Å³, *T* = 298 K, *Z* = 2. *D*_c = 1.661 g cm⁻³. *F*(000) = 488, λ(Mo Kα) = 0.71073 Å, μ = 1.435 mm⁻¹, 2θ_{max} = 47.98°, 8312 reflections measured, 3000 observed (*I* > 2σ(*I*)), 271 parameters; *R*_{int} = 0.0415, *R*₁ = 0.0318; *wR*₂ = 0.0628 (*I* > 2σ(*I*)), *R*₁ = 0.0367; *wR*₂ = 0.0646 (all data) with GOF = 1.006.